Iranian Journal of Basic Medical Sciences

ijbms.mums.ac.ir

Compromised blood-brain barrier in traumatic brain injury model of *Danio rerio*: A unique window to demonstrate restoration of behavioral, cellular, and neurochemical deficits by limonin

Juwala Malinika [1], Lalitha Vaidyanathan [1]*, Madhan Kumar Srinivasan [1], Sangeetha Chellapandi [1]

[1] Department of Biomedical Sciences, Faculty of Biomedical Sciences and Technology, Sri Ramachandra Institute of Higher Education and Research, Chennai-600116, Tamil Nadu, India

ARTICLE INFO

Article type:
Original

Article history:
Received: Aug 31, 2025
Accepted: Nov 1, 2025

Keywords:
Limonin
Microglial cell
Phytochemicals
Traumatic brain injury
Zebrafish

ABSTRACT

Objective(s): Traumatic Brain Injury (TBI) poses a significant risk factor for various neurological complications, ranging from acute manifestations in severe cases to insidious onset in mild instances, often leading to fatal outcomes with elusive aetiologies until post-mortem examination. Limonin, a secondary metabolite renowned for mitigating metabolic syndrome risk factors, notably cardiovascular complications and fatty liver disease, demonstrates promising neuroprotective properties *in vitro*. This study aimed to elucidate the *in vivo* neuromodulatory effects of limonin using an adult zebrafish model.

Materials and Methods: The compound was evaluated for toxicity to zebrafish using the comet assay and phenotypic assessment. Through a series of assays encompassing behavioral, histological, and biochemical analyses, rescue from cell death was observed in adjacent regions despite the native regenerative background of a wild-type zebrafish. A novel brain cell suspension from adult zebrafish was also employed to discover rescue against necrotic cell death cues.

Results: Lipid peroxidation-induced neuroinflammation and 2-fold reduction of free radicals, compared with TBI controls, were observed with 300 µM Limonin treatment. The cell viability assay performed, indicated at least 5-fold reduction in the cell damage due to brain injury. Histopathological sectioning and staining showed reduction in inflammatory cell infiltration and demyelination demonstrating the anti-inflammatory and neuroprotective properties of limonin. We also demonstrated behavioral changes associated with TBI that can be alleviated by limonin treatment.

Conclusion: These findings underscore the potential of limonin as a potent neuromodulator and warrant further preclinical investigations to mitigate TBI-associated neurological deficits.

▶ Please cite this article as:
Malinika J, VaidyanathanL, Srinivasan MK, Chellapandi S. Compromised blood-brain barrier in traumatic brain injury model of *Danio rerio*: A unique window to demonstrate restoration of behavioral, cellular, and neurochemical deficits by limonin. Iran J Basic Med Sci 2026; 29: 468-481. doi: https://dx.doi.org/10.22038/ijbms.2026.90876.19603

Introduction

Limonin ($C_{26}H_{30}O_8$) is a heterocyclic triterpenoid, a highly oxygenated secondary metabolite, predominantly available in citrus fruit seeds belonging to the *Rutaceae* family. The second most common source, for its abundance, is *Azadirachta indica*, a member of the *Meliaceae* family (1).

Formed from the basic precursor of Acetyl-CoA, condensation and reduction of the subsequent products formed in all levels of reaction leads to the formation of triterpenes as a consequence of the acetate-mevalonate pathway (AMP). The evaluation of these metabolites for the beneficial properties they possess enables recognition influenced by their chemical structure. This knowledge has been utilised to modify and create semi-synthetic versions of the compound, offering an added advantage over the native structure and yielding derivatives with enhanced properties, for instance, a potent anti-inflammatory agent (2). Focus on modifying the properties for betterment, for use in medicinal chemistry, is another aspect highlighting the possibility of advantageous utilization by creating derivatives. For instance, the modification of water-insoluble limonin to make it water-soluble for its unhindered use is worth mentioning (3).

Water-insoluble citrus limonoids are limonoid aglycones like limonin, but the other counterpart that exists as water-soluble ones are limonoid glucosides (4). Citrus limonoid aglycone's presence can be noted from the bitterness it causes in fruit juice after production and is hence considered a drawback in such an industry (5).

The focus on producing chemical derivatives contrasts sharply with the scant attention to this compound, primarily because of its reputation for low bioavailability. Even more reduced in the case of neurological studies for the same reason. The compound inhibits calcium influx and, hence, free radical production mechanistically. It is also hypothesized to cause an increase in expression of

***Corresponding author:** Lalitha Vaidyanathan. Department of Biomedical Sciences, Faculty of Biomedical Sciences and Technology, Sri Ramachandra Institute of Higher Education and Research, Chennai-600116, Tamil Nadu, India. Tel/ Fax: +044-2476 8027/29, Email: lalithav@sriramachandra.edu.in

neuroprotective proteins, ultimately reducing glutamate-induced neurotoxicity in primary rat cortical cells (6).

Apart from its beneficial effects in neural tissue, it has been proven to have remedial properties for systemic pathologies as well, including pharmacological effects such as anti-inflammatory, antioxidant, analgesic, anticancer, antiviral, antifungal, and antibacterial (6). Furthermore, a study using zebrafish has shown that limonin can alleviate fatty liver disease (7), demonstrating its systemic benefits. Given its broad spectrum of effects, the potential benefits in the context of brain injury are of particular interest, particularly regarding protective mechanisms at the molecular level.

Traumatic brain injury (TBI) is predominantly a silent but potent problem considering the pathologic manifestations it presents, largely with no option available for treatment of its symptoms (8, 9). Not only do severe TBIs pose a threat to a person's life, but also the mild ones slowly aggravate, creating problems later in life. Apart from mortality, those alive suffer from a lifelong inadequacy, with low quality of life, and even more threatening is the decline in emotional and cognitive abilities along with memory, presenting with a change in character.

The fundamental pathology after receiving a severe injury to the brain or with repeated mild injuries like concussions, the manifestations are subtle in some instances and worsen over time. An in-depth understanding of the molecular mechanisms and classification of injuries for each individual is crucial for providing an effective personalised treatment plan. The severity of the pathology and the diagnosis/screening of the pathophysiology to identify targets for treatment needed for patients are still under research.

In the clinical setting, mild, moderate, and severe forms of TBI are classified mainly by the Glasgow Coma Scale (GCS), duration of loss of consciousness (LOC), and/or duration of post-traumatic amnesia (PTA). So far, several preventive medications like anti-seizure drugs are prescribed along with rehabilitation to treat the symptom that comes along with the pathology to stop them from getting worse and to develop and relearn the skills lost. But with increasing knowledge obtained with research on the pathophysiology of TBI, it can be made possible to classify, diagnose, and give a reliable prognostic inference post-injury for better care, especially with mild TBI, with no definitive diagnosis attainable with the existing imaging technology, like CT and MRI, wherein the pathology can go unseen.

Some of the events that occur post-TBI excluding the neuropsychiatric events are seizure, Blood Brain Barrier (BBB) break, infiltration of systemic and immune cells with the call of native ones and subsequent inflammation (10), abnormal protein accumulation precipitating neurodegenerative diseases like Alzheimer's, Lipid accumulation and peroxidation due to increase in reactive oxygen and nitrogenous species as well as ultimate cell death, be in necrotic or programmed ones like apoptosis.

Pain, motor control deficits, and neuropsychiatric conditions are some of the symptoms that show after having incurred TBI, which are treated individually by means of medication as a part of rehabilitation, expectedly along with its own set of complications (11).

Zebrafish, which share 70% homology in their genetic makeup with humans, exhibit similarities in many pathological phenotypes, including brain injury (12). It is said that 82% of human genes associated with a disease have a zebrafish homologue and thus define the way in which the outcome progresses, if not exactly as in humans, at least *in vivo*. Given this fact and many other advantages this model has over rodents, including the area it occupies or is needed, it has been increasingly used as a model for studying neurodegenerative diseases, with valid standard protocols established for inducing the pathology. Organogenesis is complete at 92 hr post-fertilization, including the gut. Treatment and housing in a culture plate well are possible with a lower, compatible dosage of the drug, unlike that required in higher vertebrate models. Overall, reductions in scale and maintenance costs are possible compared to other behavior screening models.

In this study, the induction of TBI is anticipated to breach the BBB, allowing screening of limonin as a potentially beneficial neuroprotective phytocompound and assessing its influence on a broad spectrum of factors contributing to secondary injury. Some research claims that limonin, specifically limonin glucoside, has no antioxidant effect, which has proven controversial in oncological cases, unlike other studies on the scope of brain aging. The purpose of the study is to give a stance of the compound as a neuromodulator in an injury-incurred environment. Since most neuroprotective studies done *in vivo* and *in vitro* are with limonin pre-treatment, the concept of administration post-injury and its subsequent possible neuroprotective effect is a part of the design of this study.

Limonin's effect in cases of function against the multifaceted pathogenesis of TBI remains incomprehended and warrants exploration. The compound, as previously mentioned, is said to have neuroprotective effects and is focused on in this study in a TBI-induced adult zebrafish model to help analyze if there are any cellular, biochemical, physical, microenvironmental, and gross anatomical effects in the CNS. Heeding a direction toward the pathway of its mechanistic action, contributing to the stabilization of a few secondary pathophysiological events post-injury, is the goal.

Materials and Methods

Zebrafish husbandry

All the methodologies follow standard procedure for zebrafish maintenance and euthanasia (13).

Environmental conditions

Temperature was maintained at 25 ˚C, and aeration was provided through motor-operated air pumps. The animals were kept under a 12-hr photoperiod of artificial light and 12-hr darkness.

Housing

Animals would be maintained in glass tanks with regular tap water, with 10-15 fish per litre, and the water changed once every 2 days. Antifungal solution is mixed with the tank water (1 drop/litre) to prevent fungal infections.

Diet

Fish were fed micro-pellet fish food (commercially available) and freeze-dried worms twice a day.

Preparation of limonin concentrations

Limonin concentration of 1 mg/ml using tetrahydrofuran (THF) as the solvent was prepared, and the stock was used to disperse the chosen range of concentration into the tank containing 100 ml of tank water. THF and its biological

effects have been documented (14). The concentration range was chosen based on cumulative evidence of biologically active limonin doses reported to alleviate pathological changes in experimental models (15).

The groups considered in each assay were compared with the healthy (Sham) and the negative control (TBI control). The treated groups T1, T2, T3, and T4 correspond to the 200, 300, 400, and 500 µM concentrations, respectively. The concentration range was chosen based on cumulative evidence of the optimal dosage range that has been proven to alleviate systemic pathologies.

Toxicity studies

Oral tank water administration as part of oral gavage is a one-time administration, wherein the tank water is not changed for a period of 3 days to retain the limonin-treated water for the duration of the study.

General behavioral toxicity screening for limonin and THF solvent

Skin lesions, preference for dark tank locations, increased and swift motility compared to normal, body curvature, body balance, instant movement towards food, and stimuli (visual and vibratory) were some of the traits screened in comparison to the untreated group. Volume of THF, not exceeding 250 to 500 µl in 1 L of tank water, was tested first, followed by testing with limonin concentration as mentioned above.

Comet assay

All the reagents and solvents were of analytical grade. Replicates were performed wherever necessary. The assay was performed according to the protocol by Jarvis and Knowles (2003)(16). Briefly, slides were precoated with low-melting-point agarose (LMPA). Blood was collected from the caudal vein by centrifugation. The blood was fixed in the slide with a coverslip, followed by ethanol and buffer treatment. The slides were subjected to electrophoresis and stained with ethidium bromide to visualize the fragmented DNA.

Behavioral and phenotypic presentations

Distribution parameters, such as schooling/shoaling behavior and surface/bottom distribution, were observed and noted following a single-blinded study in which the marks or ranks were assigned by a peer unaware of the study groups. The latter parameter is seen as part of locomotion, suggesting a healthy trait. Horizontal/vertical orientation, loss of buoyancy control, spiral swimming, hyperactivity, hypoactivity, gulping, aggression, convulsions, and avoidance behavior were observed during the behavioral analysis. Changes in appearance, like irritated skin, edema, skin colour (darkening/lightening), Hemorrhage (petechiae/haematomas), and exophthalmia are also noted for assessing the toxicity of the compound (13). Appetite and response to stimulus, both visual and vibrative, are also checked.

TBI induction

TBI was induced following the standardized protocol demonstrated as Stab Wound Injury of the telencephalon (15, 16). In brief, the fish were anesthetized using a 0.4% tricaine stock solution. A 1 ml tubulin syringe needle was used to puncture the anterior region between the eyes. Fish were reintroduced into tanks again, with treatment tanks containing specific concentrations of limonin to study the dynamics of recovery.

Behavioral assessment post-TBI induction

Neurotransmitter imbalance-glutamate excitotoxicity test and pectoral fin dynamics (behavioral screening)

Evaluation of rhythmic caudal fin movement described as flicks is measured for the number of times in a continuum, the times of recurrence within two minutes, and the duration of flicks in seconds.

With caudal fin movements observed, pectoral fin movements were also noted. Possible loss of voluntary motor control was measured by means of analysing the time of onset and the duration of such movements.

NTT (novel tank test)

The fish were introduced into a new tank after induction and treatment with Limonin, and were tested at 0, 24, 48, and 72 hpi at different concentrations. The behavioral and swimming patterns of the fish were noted, along with their prevalence at the top, middle, or bottom levels of the tank, with an imaginary distinction between the levels to correlate with patterns of depression, anxiety, fear, and good health ascertained by exploratory behavior.

Intact parenchymatous evaluation (Gross anatomy)

Brain edema

Brain edema was measured using the wet-dry weight method (17). Brain tissues were dissected from the adult zebrafish and weighed using a physical balance before and after drying. All brain samples from different groups isolated at 24 hpi were kept in a hot air oven (60 ˚C) for 4 hr (18). Hot plates were not used for fear of burning tissue. The formula to calculate the water content is as follows:

$$\% \text{ Water content} = 100 * (\text{wet weight} - \text{dry weight}) / \text{wet weight}$$

Brain hemorrhage

The validation of brain hemorrhage induction was done by observing the fresh isolated brain under a stereo zoom microscope (Nikon SMZ-745).

Biochemical tests

All the reagents and solvents used were of analytical grade. Replicates were performed wherever necessary.

Tissue homogenate preparation

Homogenate was prepared following the protocol by Mazzolini *et al.* (2006)(19). Briefly, zebrafish were euthanized using 4% tricaine. The brain was dissected and homogenized with 500 µl ice-cold PBS. The crushed tissues were transferred to microcentrifuge tubes and spun at 14000 rpm for 15 mins at 4 ˚C. The supernatant was separately collected, and aliquots were prepared and stored at -20 ˚C for future use.

TBARS assay/Lipid peroxidation

Zebrafish brain homogenate was prepared according to the procedure mentioned above. Assay was performed following the protocol by Visavadiya *et al.* (2016) (20). Briefly, 20 µl of the homogenate was taken in a microcentrifuge tube. To this, 40 µl of the TCA/TBA/HCl reaction mixture was added. The tubes were placed in a boiling water bath for 10 mins. The tubes with precipitate were centrifuged for 10 mins at 7000 rpm. The supernatant was transferred to the wells in the 96-well plate for reading in the spectrophotometer. The absorbance of the solutions was measured in a spectrophotometer at 540 nm.

Bradford assay/protein kinetics over chosen time-points

The Bradford Assay (21) was performed according to the protocol described by Gotham *et al.* (1988)(22). Briefly, the homogenate was aliquoted, and 5ml of Bradford's (acidified Coomassie brilliant blue) reagent was added. The blue colour so formed was measured spectrophotometrically at 595 nm.

Histopathological analysis

Horizontal sections of 10 microns from the isolated brain parenchyma of every group were used to perform this analysis.

H&E/ immune cell types and their infiltration

Staining was performed based on the protocol developed by Cardiff *et al.* (2014)(23). Briefly, the tissues fixed in 10% formalin were processed and stained with haematoxylin, followed by eosin to stain the nucleus and cytoplasm, respectively. H&E staining was not intended to provide definitive classification of neuronal versus glial populations, but rather to offer histological context regarding the overall neuroinflammatory state.

Luxol fast blue/demyelination

Staining was performed according to the protocol described by Goto (1987) (24). Briefly, the tissue sections were immersed in Luxol fast blue overnight, followed by alcohol treatment; further counterstaining with lithium carbonate provides clear contrast.

Oil red O/lipid droplets

Sections not exposed to clearing solvents were deparaffinized and stained with Oil red O, according to the protocol described by Koopman *et al.* (2001)(25), to visualize lipid droplets. No alum haematoxylin was added to stain the nuclei. Staining intensity was used to assess differences between the control and treated groups.

Cell death assay

Preparation of the zebrafish adult brain whole cell suspension was standardised for the first time and stained with AO/EB to observe apoptotic populations.

Cell suspension preparation

Brain tissues of the fish were dissected and homogenized mildly using a mortar and pestle. The brain was mildly homogenized again with 200 µl of Media A and centrifuged for 20 mins at 300 rpm at 4 ˚C. The supernatant was separated and centrifuged for 10 mins at 5000 rpm at 4 ˚C. The supernatant was discarded, and the pellet was resuspended in 10 µl of Media A (19).

Comparison of the presence of apoptotic and necrotic cells

The resuspended pellet of cells was taken, and 2 µl of AO working solution and 2 µl of EB working solution were added and incubated for 5 mins in the dark. The sample was mixed, 5 µl was taken and placed in a single well, and a round coverslip was placed on top to form a monolayer of cells. This setup was viewed under an inverted microscope to visualize and count the percentage of dead (red, yellow-green, and orange, indicating necrotic and early- and late-apoptotic cells, respectively) and live cells (green).

Pro-apoptotic (Bax) and Pro-inflammatory cytokine (IL-6) expression analysis

The gene expression analysis was performed on brain tissue. The tissues were homogenized and enzymatically treated to extract RNA. The RNA was converted to cDNA and then subjected to the polymerase chain reaction.

Isolation of total RNA

Using a total RNA isolation reagent (TRIR) kit, total RNA was extracted from both control and test samples/ In summary, 1 ml TRIR was used to homogenise 100 mg of fresh tissue. The homogenate was then quickly transferred to a microfuge tube and maintained at -80 ˚C for 60 min to allow nucleoprotein complexes to dissociate fully. Following a one-minute vortex and a five-minute cooling period on ice at 4 ˚C, 0.2 ml of chloroform was added. The homogenates were centrifuged for 15 min at 4 ˚C at 12,000 x g. After carefully moving the aqueous phase into a new microfuge tube, the same volume of isopropanol was added, vortexed for 15 sec, and the tube was kept on ice at 4 ˚C for 10 min. The samples were centrifuged for 10 min at 4 ˚C at 12,000 x g. After discarding the supernatant, the RNA pellet was centrifuged for 5 min at 7500 x g (4 ˚C) after vortexing and washing with 1 ml of 75% ethanol. After removing the supernatant, the RNA pellets were mixed with 50 µl of autoclaved Milli-Q water and heated in a water bath at 60 ˚C for 10 min to dissolve.

Quantification of RNA

The absorbance (A) at 260/280 nm was measured spectrophotometrically to quantify the diluted RNA sample. One absorbance unit at 260 nm is obtained with 40 µg of RNA in 1 ml. Therefore, by multiplying the A260 of the sample by 40 and the dilution factor, one can determine the concentration of RNA in the given sample. The ratio of an RNA preparation's absorbance at 260 and 280 nm can be used to determine its purity. A 260/280 nm absorbance ratio greater than 1.8 is commonly regarded as indicative of high-quality RNA. The obtained RNA has a purity of 1.8.

The tubes were carefully mixed, quickly spun, and then placed in the thermocycler, which was set to begin the reaction at 25 ˚C for 10 min, initiate the reverse transcriptase reaction at 48 ˚C for 30 min, and inactivate the enzyme at 95 ˚C for 5 min.

The CFX96 Touch Real-Time PCR Detection system from Bio-Rad CA was used to perform real-time PCR. 5 µl of 2X reaction buffer, 0.1 µl of sense and anti-sense primers, 1 µl cDNA, and 3.8 µl of sterile water were added to create the reaction mix (10 µl). The temperature cycler protocol was as follows: 3 min of initial denaturation at 95 ˚C, followed by 40 PCR cycles with denaturation at 95 ˚C for 10 sec, annealing at 60 ˚C for 20 sec, and extension at 72 ˚C for 20 sec.

Every reaction was carried out in triplicate without a template control (NTC). Melt curve analysis was used to identify the presence of numerous amplicons, non-specific products, and contaminants. Thermal cycling was programmed at 50-95 ˚C for each sample. The CFX96 Touch Real-Time PCR Detection System from Bio-Rad was used to evaluate the data. Fish β-actin was used as an invariant control in this investigation.

Statistical analysis

Results were analysed and numerically represented as mean±SD. Tests such as Ordinary Two-way ANOVA were performed to compare all TBI-induced groups, including the negative TBI control and treated groups. The specific tests used are listed in the legends for the assay graphs.

One-way or Two-way ANOVA tests were performed depending on the groups compared, excluding or including the negative control group (TBI untreated), respectively. Data analysis was performed using GraphPad Prism, and *P*-values<0.05 were considered statistically significant. Biological replicates of N=3 were included in this study for each experimental condition for each assay conducted.

Results

No toxicity indication for limonin and tetrahydrofuran (THF) tested through behavior

No distinct differences or mortality over a course of 72 hr were observed in the behaviors noted, compared with the untreated group, for either THF alone or in combination with limonin, suggesting promise within the chosen range. The maximum quantity of THF chosen to be used as a solvent was 300 ppm, which is within the maximum tested concentration of 500 ppm. At lower concentrations, all showed no skin or eye irritation, as reported in the literature as manifestations of toxic dosage.

Absence of DNA fragmentation in the comet assay up to the highest concentration of limonin

To determine the appropriate concentration range to study, the maximum value within the range is selected to assess DNA fragmentation. No comets were observed post-treatment, suggesting that no breaks were introduced into the genetic material.

The chosen range demonstrates no discernible extremes of toxic manifestations post-injury, as validated through meticulous behavioral screening encompassing locomotion, appetite, and response to stimuli.

No abnormal behaviors or manifestations were observed following exposure to limonin concentrations in relation to post-injury effects. Through visual single-blinded screening, behaviors such as appetite, coordinated locomotion, and response to stimuli were graded, revealing no abnormalities. Additionally, no mortality or skin lesions were observed in any of the test groups. Feeding behavior returned to normal in the TBI-induced group, and the fish resumed free swimming after 2 min, following the standard protocol established by Schmidt (2014)(16). Consequently, test groups exposed to concentrations of 200, 300, 400, and 500 µM were confirmed not to be toxic. Notably, the T2-treated group of 300 µM exhibited behavior closest to that of Sham.

Neurotransmitter imbalance

The behaviors observed, closely related to brain injury, such as fin movements and motility patterns in zebrafish, were empirically measured. Due to the lack of behavioral monitoring systems, a 30-minute screening time was implemented across all groups.

A standardized observational test, examining caudal and pectoral fin dynamics, reveals correlations with seizure-related spasms. At the same time, concurrent observations of neuropsychiatric behaviors suggest a potential neurotransmitter imbalance, which is reduced with treatment.

Caudal fin dynamics

The caudal tail dynamics reflecting aberrant neuronal firing resulting from elevated levels of neurotransmitters, particularly glutamate, could be reduced in the T2 group (Figure 1A).

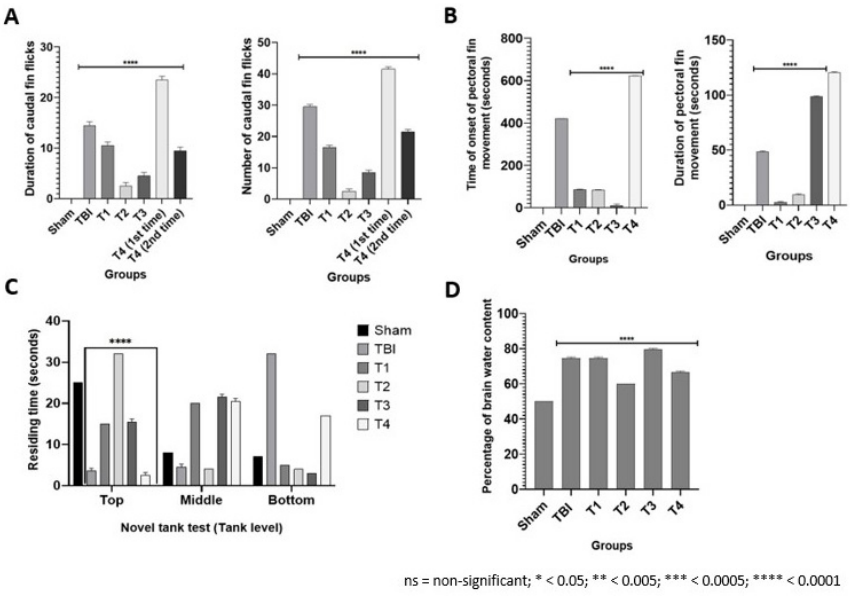

Figure 1. A) Caudal tail flicks/spasm. Duration and the number of the spasm were measured by counting the seconds and the number of flicks, respectively, after onset. Significant differences between groups were found using a two-way RM ANOVA. **** ascertains the effect of limonin and the difference of the same across different groups of T1, T2, T3, and T4, corresponding to 200, 300, 400 and 500 µM of Limonin. T2 shows the shortest duration of flicks and the number of spasms compared to any other concentration, with a mean value of 2.5+ ± 0.707 and 3+ ± 1.414, respectively. B) Rhythmic pectoral fin movement with no forward motion. The two-way ANOVA shows a significant difference between the untreated and treated groups. The duration of movement is shorter in both the T1 and T2 groups, whereas it is longer in the T3 and T4 groups. Onset seems to occur later in the TBI group, unlike in the T1, T2, and T3 (10.5±6.364) groups, with a much-amplified presence in the T4 group, suggesting a possible harmful disposition. T1 seems much more effective at controlling the duration of such rhythmic motion, with a mean value of 2.5±0.707 sec, compared to 9.5±0.707 in T2. C) NTT graph. Duration of location of fish (in seconds) at the three imaginary levels of the tank at 0 hpi. Two-way ANOVA was performed between the TBI and treated groups; **** indicates a significant difference in anxiety between the untreated and treated groups, with a marked decrease in anxiety in T2, with a mean residence time of 30.5±2.121 sec at the top level. D) Brain edema was measured at 72hpi, post-definite occurrence of hemorrhagic effects by estimating the % water content. **** estimated by two-way ANOVA. T2 had markedly less percentage of water content with a value of 60, with no standard deviation

Pectoral fin dynamics

Pectoral fin dynamics, as documented by Tiedeken *et al.* (2005)(26), were also observed alongside caudal fin movement to assess overall swimming ability and indicate motor control and validate glutaminergic neuronal control (27) in TBI. Prolonged, rhythmic, and repetitive circular tick-like movements on one side, persisting without variation throughout the observation period, suggest potential involuntary motor disruption, a characteristic seen in the TBI group. These movements exhibit a delayed onset and persist for an extended duration, lasting around 48 sec. In contrast, the treated groups T1 and T2 display earlier onset and shorter duration of such movements, with T3 showing similar patterns except for duration. T4, however, shows no improvement compared to the TBI group (Figure 1B).

Since the survival rate in this study is 100% after the induction protocol, interpretations are based on relative results compared with the TBI group. Compared with the groups, mitigating diffuse neurotransmitter imbalance and reducing seizure-like activity duration closely align with improving outcomes.

Novel tank test (NTT)

The novel tank test (NTT) serves as a standard assessment tool to evaluate the neuropsychiatric condition in the TBI-induced model. Fish treated with 300 µM concentration from the T2 group displayed anxiety levels and exhibited exploratory behavior by venturing to the top levels of the tank, mirroring the behavior of healthy fish at 24 hr post-injury (hpi). Conversely, fish in the TBI control group displayed depressive behavior by persisting at the bottom level of the tank with minimal response to stimuli. However, fish from the T2 group gradually moved to the top level over time, indicating the overcoming of chronic anxiety post-head trauma, as depicted in Figure 1c. Notably, the cumulative consensus of behavior is significantly different from that of the TBI group in the T2 cohort.

Gross brain anatomy

Resolution of brain edema caused by loss of vascular integrity with no exacerbation with treatment post-injury

The implemented protocol effectively prevented burnt parenchyma due to the employed drying method. Upon isolating brains from zebrafish of equal size across Sham, TBI control, and treated groups with varying concentrations, notable differences in brain size were observed. Among these, the T2-treated group at 300 µM exhibited 60% fluid retention. This suggests that the T2 group exhibited significantly lower fluid content, closer to the average of 50% found in healthy fish brains, compared to both the other treatment groups and the TBI control group (Figure 1D).

$$\% \text{ Water content} = (\text{Wet weight} - \text{Dry weight})/\text{Wet weight} * 100$$

Brain hemorrhage due to breakdown of the BBB and validation of vascular disruption, along with the potential of limonin as a possible haemostatic agent

Hemorrhage emerges as an immediate consequence following injury, with subarachnoid hemorrhage being a prevalent and perilous form, often associated with accidents in humans. Notably, the most visible reduction in hemorrhagic manifestations was observed in groups T2 and T3 (Figure 2D and E, respectively). Group T2 displays a localized spot indicative of injury, while no such spots were observed in T3. Conversely, T4 exhibited a more diffuse appearance of haemorrhagic parenchyma. Based on gross comparisons, T1 and T2 were superior at mitigating the immediate effects of hemorrhage.

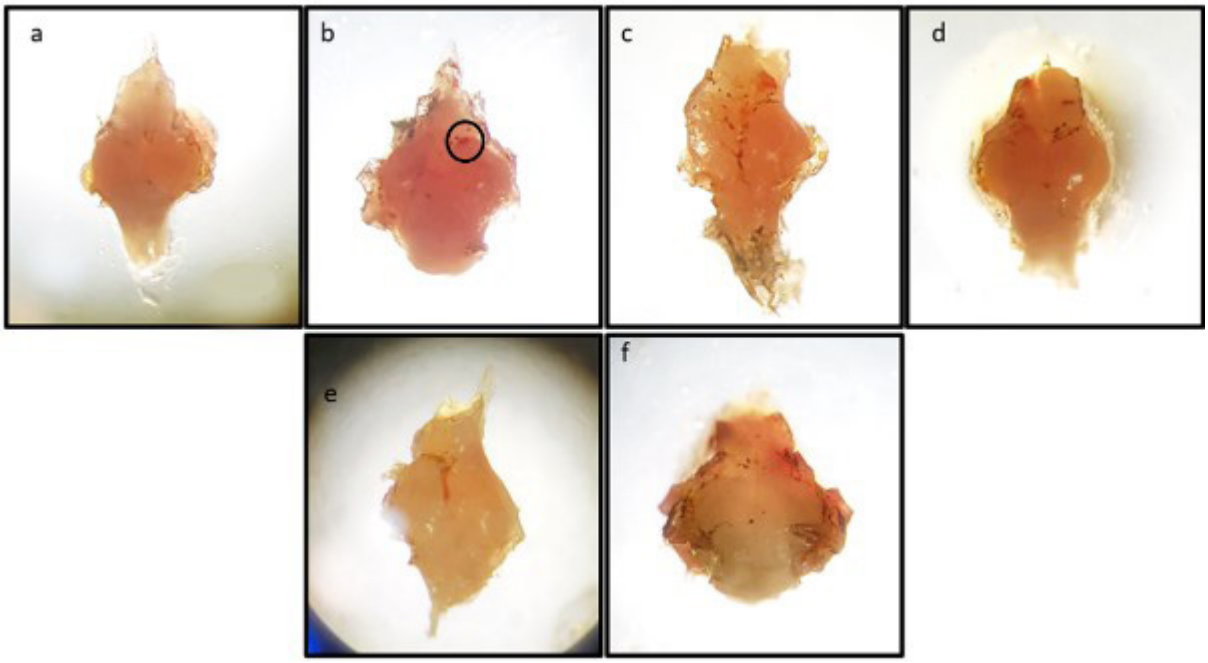

Figure 2. Brain hemorrhage in zebrafish

Brain parenchyma samples at 24 hpi of the study groups and their visual comparison. Picture description: (a) Sham, (b) TBI control, (c) T1 - 200 µM, (d) T2 - 300 µM, (e) T3 - 400 µM, and (f) T4 - 500 µM. Gross phenotype with red spots or diffuse blood suggests focal injury caused by a stab wound in the right telencephalon, and its subsequent reduction with treatment, at least showing restricted spread, can be seen

Proof of influence against oxidative stress

Validation of T2 as an optimal concentration through malondialdehyde-mediated estimation of oxidative damage in TBI

With treatment in the central nervous system (CNS), the cell homogenate obtained from post-injury samples reveals notable findings. Specifically, the T2 group treated with 300 µM demonstrates a significant reduction in malondialdehyde (MDA) levels at 48 hpi, the maximal time point studied, while still exhibiting persistent expression. Conversely, the T1 group exhibits an increase in MDA levels post-injury. Notably, among all the treatment concentrations, the T2 group displays the most favourable outcome (Figure 3).

Deciphering post-injury microenvironmental morphology

Insights from H&E staining on tissue and cellular morphology, immune cell infiltration, and nature of cell injury observed between 24 hr and 72 hr treatment period with concentrations of 200 µM and 300 µM in comparison with controls.

From Figure 4, it is evident that a slight increase in the number of microglial cells per square at 72 hpi suggests the presence of neuroinflammation following the injury. The administration of limonin appears to result in a reduction in the number of microglial cells, accompanied by a noticeable decrease in neuronal degeneration and edema. This reduction is particularly apparent in the T2 group treated with 300 µM. Notably, this group exhibits optimal effects in preventing cell swelling due to edema, thereby reducing vacuolization. The correlation between edema and neuronal degeneration suggests a potential direct relationship, as the number of microglial cells does not exhibit a consistent pattern with cell death.

Furthermore, the presence of astrocytes may indicate a pathological pattern associated with delayed recovery from neuron-glial degeneration, as evidenced by their prevalence in the TBI group at 48 and 72 hpi. Conversely, the T1-24 group and, notably, the T2 group show minimal astrocyte presence across all time points, indicating the efficacy of limonin in accelerating recovery following injury.

The findings from Figure 5 indicate early astrocyte involvement at 24 hpi, as evidenced by their presence in the T1 group. Conversely, the T2 group shows no astrocyte involvement in the inflammatory response.

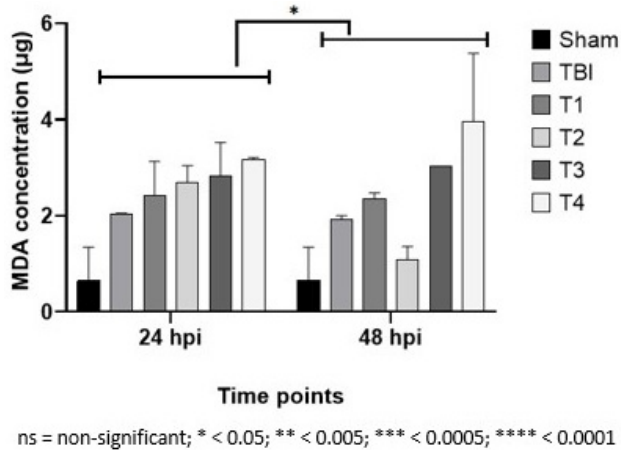

Figure 3. Concentration of malondialdehyde (MDA) suggestive of oxidative damage

T2 group shows a distinct reduction at 48 hpi from 24 hpi with a value of 1.082±0.280 from 2.691±0.354, showing a larger decrease in MDA concentration with time, unlike the other treated groups. TBI also indicates a decrease from 2.039±0.016 to 1.925±0.076 at 24 and 48 hpi, respectively. Two-way RM ANOVA suggests a difference of values among all TBI-induced and treated groups, with a *P-value* of <0.0387 denoted by *. The concentrations of groups T1, T2, T3, and T4 are 200, 300, 400, and 500 µM, respectively. The animal model used and the cohort design in all figures are adult zebrafish (*Danio rerio*)

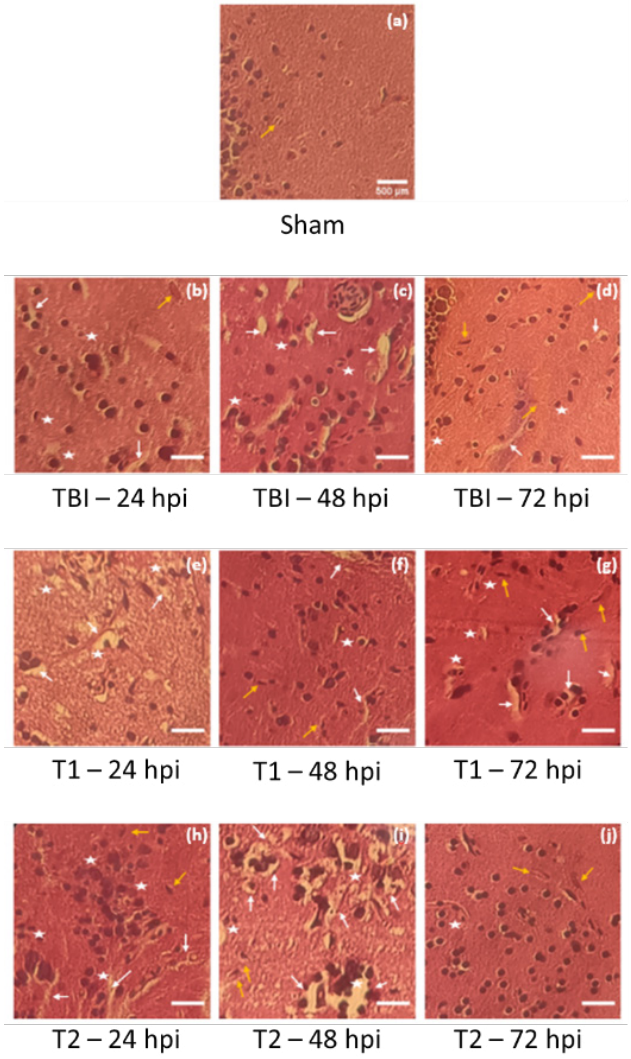

Figure 4. H&E staining of 10 µm horizontal sections of zebrafish CNS and screening for the presence of edema and its correlation with microglial cells and neuronal or glial cell degeneration

(a) Sham validates the presence of microglial cells even in non-pathological conditions. (b) TBI-24 shows no pronounced signs of dendritic and axonal swelling along with microglial cells, unlike in 48 and 72 hpi, as seen in (c) more than (d), respectively. Axonal swelling is more significant in (c) and the presence of microglial cells than in (d). (e) T1-24 has shrunken neuronal cells present in the vicinity and degenerating neurons with pallor, presenting neuropil marked due to edema, more dendritic than axonal, unlike at 48 hpi (f) and 72 hpi (g), where minimal signs of edema and specifically axonal swelling with no pallor manifestation of the tissue. Karyorrhectic neuronal cells with fewer microglial cells at 48 hpi than at 72 hpi are seen in comparison. In T2 (h), (i), and (j), no change in microglial cells was seen; however, the extent of oedematous tissue varies, with much more pronounced pathology, with degenerating cells seen at 48 hpi (i). (h) T2-24 presented with prominent Axonal swelling with two noticeable morphologies of pyknotic nucleus and eosinophilic cytoplasm of degrading neurons. T2-48 shows prominent neuronal degeneration with axonal and dendritic swelling and microglial activation. T2-72 shows microglial cells and round circumscribed neuronal cells with fewer signs of degeneration. No prominent Axonal or dendritic swelling. [White Star - degenerating neurons, White arrow - dendritic or axonal swelling which signifies edema, and yellow arrow - microglial cells. The markings in the pictures are not an exhaustive representation of all the cells within the area, but rather a general indication of the entities found overall. Images –10X magnification; Scale bar: 500 µM]. The animal model used and the cohort design in all figures are adult zebrafish (*Danio rerio*)

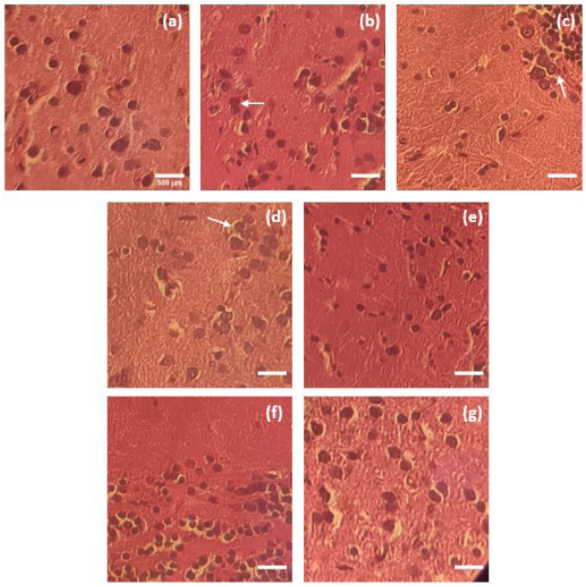

Figure 5. Astrocytes and their presence based on morphology observed in zebrafish H&E-stained brain tissue sections at 24 and 48 hpi in comparison to the TBI group, showing the involvement of astrocytes only after 24 hpi
(a) TBI-24; (b) TBI-48; (c) TBI-72; (d) T1-24; (e) T1-48; (f) T2-24; (g) T2-48. Images are of 10X magnification. Scale bar: 500 µM. The animal model used and the cohort design in all figures are adult zebrafish (*Danio rerio*)

Revealing neuroinflammation dynamics: Exploring microglial and astrocytic involvement via IL-6 Pro-inflammatory biomarker and transcriptional expression analysis

IL-6, known for its high expression during inflammation, was specifically tested in brain homogenate samples from the T2 group, relative to both the TBI and sham groups. RT-PCR analysis was conducted to accurately quantify the expression levels of the marker, even in non-pathological conditions, and to compare its abundance in pathological states relative to normal conditions.

Remarkably, the highest expression was observed in the treated groups receiving 300 µM at 48 hpi, surpassing both the sham and TBI groups (Figure 6).

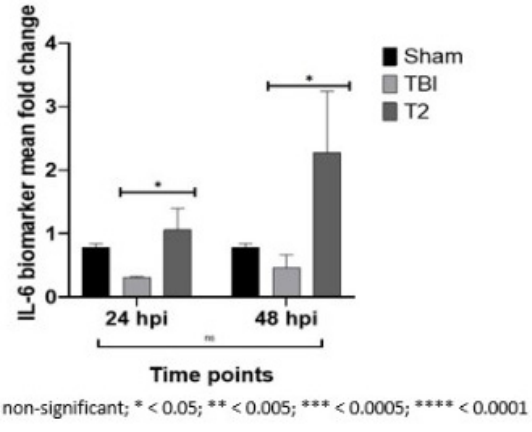

Figure 6. Pro-inflammatory marker IL-6 and its expression across the 24 and 48 hpi, a comparison between TBI and T2 zebrafish groups
An Ordinary Two-way ANOVA test shows a *P-value* of 0.0250 across the TBI and T2 groups, denoted by *, indicating the significance of the limonin effect. But across the time points, the difference in the mean increase of the marker is not statistically significant. When the TBI group shows a slight increase in IL-6 levels from 0.302±0.022 to 0.463±0.200 from 24 to 48 hpi, respectively, the T2 group shows a substantially larger increase from 1.059±0.337 to 2.278±0.963 from 24 to 48 hpi, respectively. The concentration of the T2 group is 300 µM. The animal model used and the cohort design in all figures are adult zebrafish (*Danio rerio*)

Illuminating dynamics of CNS myelin density: Enhanced levels in the T2 group after 48 hpi amid excessive inflammation across all treatment groups

Given the challenge in distinguishing spinal sections, this study focused on the telencephalon and its surrounding areas. Demyelination is notably evident in tissue sections from the TBI control group, as confirmed in Figure 7d, corresponding to the timeframe of tissue integrity loss due to inflammation, as indicated by the increase in IL-6 transcription at 48 hpi.

Among all sections observed, particularly at 24 and 72 hpi, the T2 concentration shows a protective effect against demyelination, with minimal evidence of demyelination persisting throughout the observed timeframe. Expectedly, the TBI group demonstrates low myelination intensity, consistent with the sham group. Conversely, the T2 group shows promising results, displaying optimal myelination significantly better than any other group.

Within the 72-hour timeframe, during which inflammation exerts a notable influence, particularly

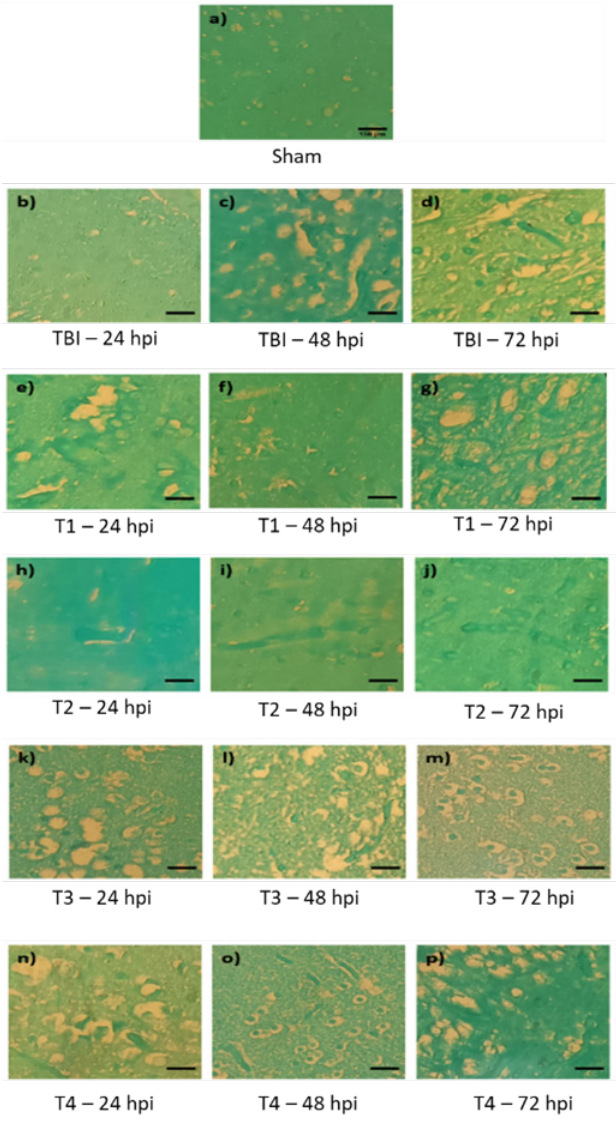

Figure 7. Visualization of evidence of demyelination post-injury in all treated and untreated zebrafish groups in Luxol fast blue staining
Demyelination is seen as spots of non-blue structures that lack stain. Images are of 40X magnification. Scale bar (a-p) is 150 µM. The animal model used and the cohort design in all figures are adult zebrafish (*Danio rerio*)

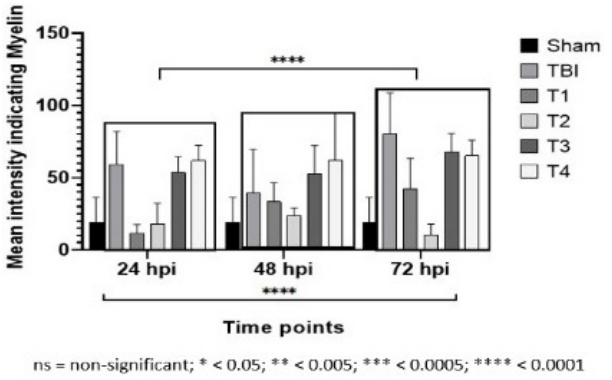

Figure 8. Grey scale value indicative of the myelin staining intensity across all studied zebrafish groups across 24, 48, and 72 hpi
ImageJ software assembled, and GraphPad Prism analysed the data graphically, showing that the lower the grey value, the closer it is to the purest colour chosen to be measured across all groups against the background colour, preventing its interference. In terms of myelination, the T2 group shows greater effectiveness than the other treated groups, with mean intensity values of 17.92±14.39, 23.86±5.22, and 10.34±7.50 at 24, 48, and 72 hpi, respectively. Although T1 groups show better protection against demyelination at 24 hpi than T2, over time, T2 maintains myelin content and can thus be considered the optimal concentration. An Ordinary Two-way ANOVA test performed with a *P-value* of <0.0001, as denoted by ****, validates the mean intensity values across all groups (as seen above) in correlation with the different concentrations across different time points and their effects. The animal model used and the cohort design in all figures are adult zebrafish (*Danio rerio*)

evident at 48 hpi with increased IL-6 levels in the T2 group, the loss of myelin is not pronounced or deleterious. Instead, myelin preservation is observed, particularly at 72 hpi, with a significant difference observed across time points (Figure 8)(Brown-Forsythe ANOVA and Welch's ANOVA test, *P*-value<0.0001).

Screening for biochemical dynamics

Lipid droplets: Key players in neuropathogenesis and myelination dynamics post-injury, with T2 demonstrating significant reduction amid chronic inflammation and favourable phenotypic changes

Focusing primarily on regions in and around the telencephalon, our observations reveal a notable decrease in lipid droplet content over time in the T2 group at a limonin concentration of 300 µM. This reduction is associated with lower fluctuations in mean intensity compared to the TBI control group at 48 hpi (Kolmogorov-Smirnov test; *P*-value<0.0001) and to the sham group. Our analysis indicates that T2 exhibits a protective effect against lipid droplet accumulation during the 24-48 hr period post-injury, with T1 also showing a gradual decrease in lipid content, albeit with a higher standard error of the mean and a manifestation of clustered lipid droplets. Lipid droplets contain a significant proportion of polyunsaturated fatty acids (PUFAs), which play a crucial role in remyelination. Interestingly, lipid droplet accumulation decreases in the T2 concentration group at 72 hpi, approaching levels observed in the sham group. While the TBI and T1 groups at 72 hpi (Figure 9g) appear darker, indicating a higher lipid content, this was not validated by intensity measurements due to the lack of uniformity in this distinctive feature across all groups.

Given lipid droplets' role in regulating microglial reactivity and the potential for chronic inflammation and scarring with prolonged microglial presence, effective control of lipid accumulation is imperative. Our findings suggest that the optimal time for lipid reduction is around 72 hpi, coinciding with the need for immune cell activity.

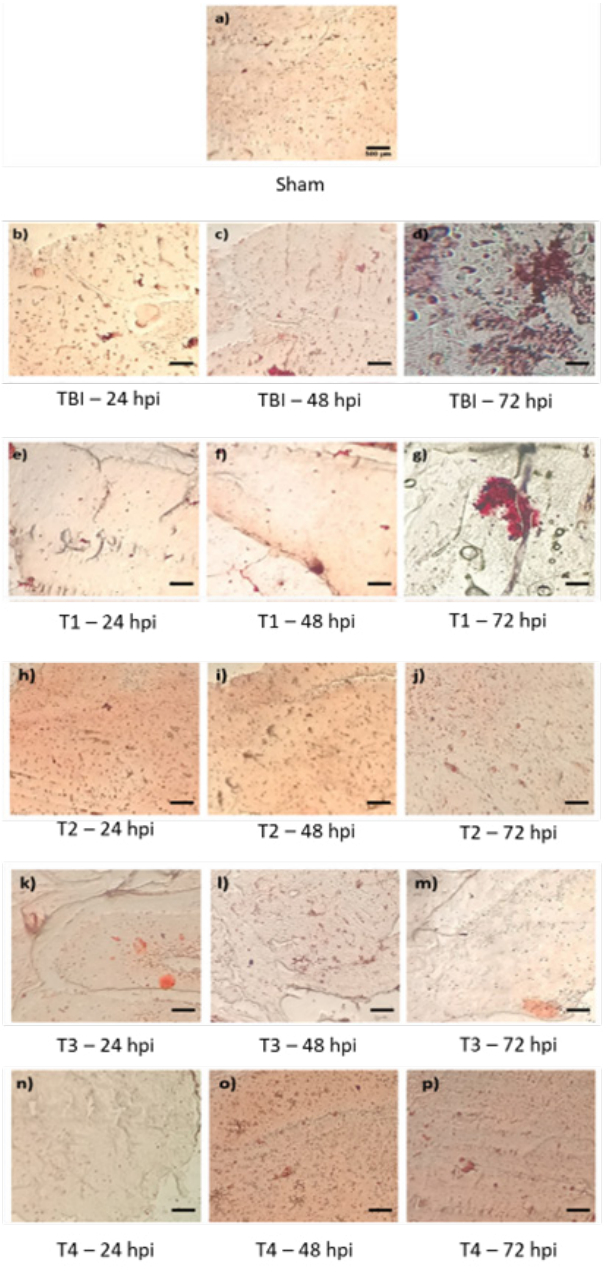

Figure 9. Oil red O staining for the treated and untreated zebrafish traumatic brain injury (TBI) groups, along with Sham having TBI at 24, 48, and 72 hpi
The group sections exhibit diffuse lipid droplet distribution, not restricted to the focal area of traumatic injury. The image is of 10X magnification. Scale bar (a-p) is 500 µM. The animal model used and the cohort design in all figures are adult zebrafish (*Danio rerio*)

T2 concentration shows a pronounced decrease in lipid accumulation across the three time points studied (Figure 10), indicating its potential to prevent exacerbated immune cell reactivity and promote tissue repair. In contrast, T1 shows patterns similar to those of the TBI group, with signs of demyelination persisting at 72 hr, highlighting the potential deleterious effects of excessive lipid reduction on myelination.

Bradford assay confirms a decrease in protein levels as beneficial for preventing the progression of secondary injury

Among the treated groups, T1 and T2 are considered

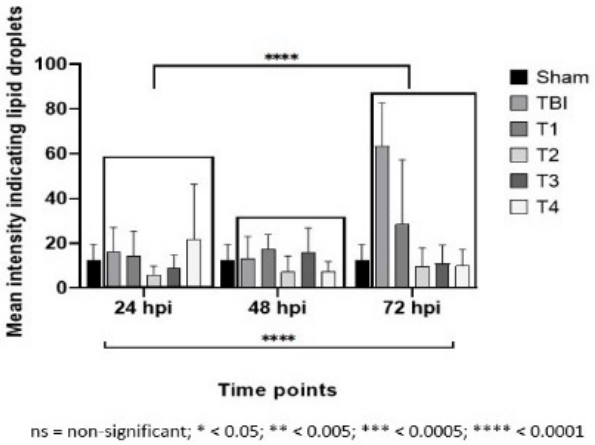

Figure 10. Grey scale value indicative of the lipid droplets intensity by means of Oil red O staining across all studied zebrafish groups across 24, 48, and 72 hpi

The least fluctuation in oil droplet intensity across time points, relative to sham, is observed in the T2 group, with the purest colour threshold filtered value and acceptable SD. Notable but subtle increase in lipids with mean intensity values of 5.834±3.999, 7.246±7.109, and 9.484±8.422 from 24, 48, and 72 hpi, respectively, is seen in T2, which could be an optimal effect in correlation with all other studies done ascertaining the efficacy of 300 µM concentration. The animal model used and the cohort design in all figures are adult zebrafish (*Danio rerio*)

adequate, with stable protein content and minimal fluctuations. While a decrease in protein content is generally considered detrimental to the overall prognosis in the context of neurodegenerative diseases, the significance of a general, unspecified estimation of proteinaceous content lies in its potential to reflect the post-injury activity of molecular machinery. The subtle decrease in protein content observed in the TBI group compared to the sham group may suggest reparative activity, a natural ability observed in wild-type zebrafish post-injury (Figure 11). Following assessments of neuroinflammation, myelination, and oil droplet accumulation, the slight decrease in protein content observed in the T2 group, similar to that in the TBI

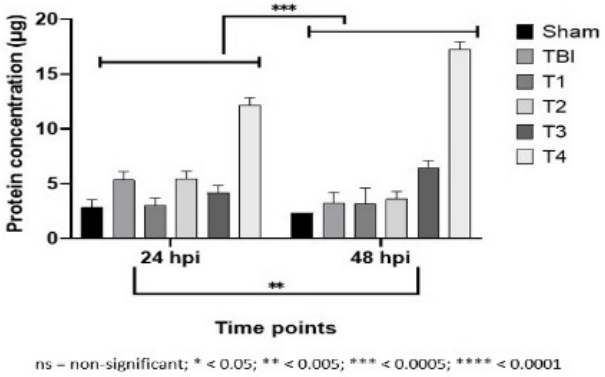

Figure 11. Bradford assay to measure the basal non-specific protein concentration across 24 and 48 hpi in zebrafish

The assay shows a significant difference among all TBI-induced groups, as determined by Two-way ANOVA. Decreases in protein levels in traumatic brain injury (TBI) are from 5.343±0.757 to 3.206±0.990, and in T2 from 5.437±0.7.7 to 3.577±0.707 at 24 and 48 hpi, respectively, suggesting a post-injury effect, not necessarily sequential, of proliferation, inflammation, and ultimate cell death. The animal model used and the cohort design in all figures are adult zebrafish (*Danio rerio*)

group, may indicate a correlation between protein levels and pathological processes.

Across the 24 and 48 hpi time points, T2 demonstrates a reduction in protein content akin to the regenerative effect observed in native zebrafish post-stab injury, albeit in a much shorter timeframe than previously studied. In line with improvements in pathology parameters at 72 hpi, the protein levels in the T2 group are considered conducive to recovery.

Cellular degeneration

Evaluating cell degeneration and viability using EtBr/AO staining in isolated brain samples

Necrosis, characterized by uncontrolled cell death and the release of intracellular constituents, can precipitate multiple devastating secondary injury events. However, we observed no evidence of mass necrotic death in the treated group, unlike in the TBI group at 24 hpi (Figure 12b). At 24

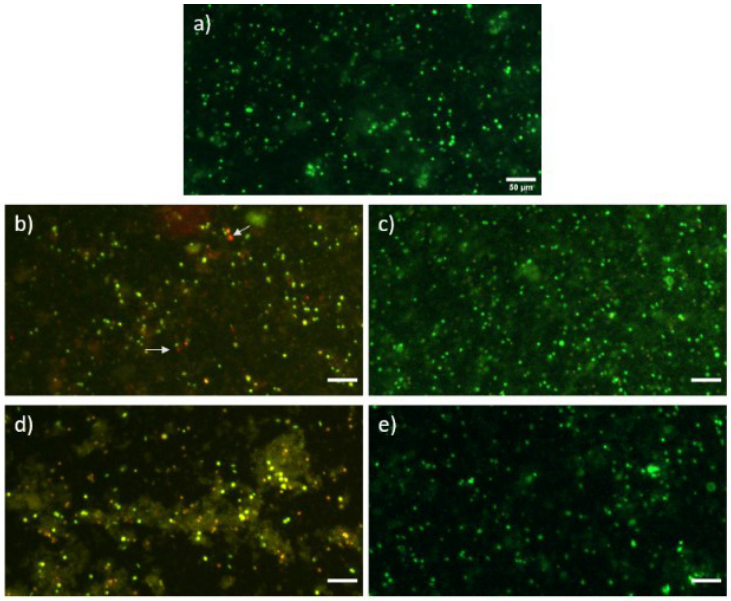

Figure 12. Acridine orange /ethidium bromide (AO/EB) staining of neural cells procured from the zebrafish traumatic brain injury (TBI) induced and subsequently treated groups of one possible effective 300 µM concentration

Apoptosis appears evident, as seen in cells with hues of yellow-green and orange. Red spots show marked means of necrotic death as seen at 24 hpi without treatment in (b). Image magnification at 10X. (a) Sham; (b) TBI 24 hpi; (c) TBI 48 hpi; (d) T2 24 hpi; (e) T2 48 hpi. Scale bar (a-e) is 500 µM. The animal model used and the cohort design in all figures are adult zebrafish (*Danio rerio*)

hpi, early apoptotic and late apoptotic cells, distinguished by distinct hues of yellow-green and orange, respectively, were visible in both TBI and T2 groups, but not at 48 hpi. Furthermore, in the TBI sample, the innate response to cell death appears to be complete by 48 hpi, indicating microenvironmental recovery by 72 hpi, as evidenced by histopathological sections.

To account for variables such as staining intensity and cell confluency within each group, the particle analyzer tool in ImageJ is used for image processing. By splitting the image into red and green channels, an objective structure count is obtained from its normalized and thresholded binary format. The ratio of red and green signals, which creates the appearance of yellow and orange hues, is calculated by normalizing the data within each group based on the total cell count (Red or Green cell count/ Total cell count in that group * 100) and normalizing between groups using the control (Total number of red or green cell count in test groups/ Total red or green cell count in control * 100).

Directional estimation of increase or decrease in cells shows a 0.88X reduction of dead cells at 48 hrs in the treated group (T2), along with maintenance of viable cells compared to the control (Table 1). A graphical representation of Table 1, indicative of the fold change, can be seen in Figure 13.

Transcriptional validation of cell death pathways: Pro-apoptotic gene expression in concordance with AO/EB staining

Analysis of the differentially expressed Bax gene was conducted using a set of primers (5′-3′) forward primer – CCGTGAGATCTTCTCTGATGG and reverse primer – GTCAGGAACCCTGGTTGAAA. T2, identified as the optimal concentration in many assays conducted herein, was utilized to estimate its differential expression as a result of limonin at 24 and 48 hpi, both time points known for maximal dynamics, especially pertaining to apoptosis (Figure 13).

A visible reduction at 48 hpi in the T2 group compared to the TBI group in Figure 14, in line with the AO/EB staining results (Figure 12) and inflammatory signals, further validates T2's effectiveness in reducing cell death and, hence, apoptosis.

Table 1. Directional estimate of zebrafish dead/viable cells from AO/EB assay

Cell count	TBI-24	TBI-48	T2-24	T2-48
Red	18.68	1.44	19.31	0.88
Green	0.5	0.98	0.48	1

Greater than 100% indicates an increase in cells relative to the control, and less than 100% indicates a decrease. Green indicates viable cells (acridine orange-positive), while red indicates dead cells (ethidium bromide-positive)
TBI: Traumatic brain injury

The validity of T2 at 48 hpi, along with interpretations from H&E and AO/EB staining, suggests significant anti-apoptotic activity, given its proximity to sham levels. However, due to the minute differences in values, no empirical significance could be determined.

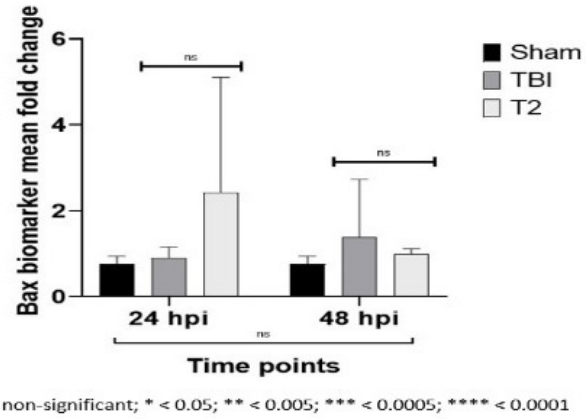

Figure 14. Pro-apoptotic biomarker of Bax and its transcriptional expression across the 24 and 48 hpi samples of zebrafish traumatic brain injury (TBI) and T2 group
Increase in Bax transcript expression from 0.899±0.254 to 1.374±1.351 in the TBI group and a decrease from 2.420±2.683 to 0.992±0.124 in the T2 group from 24 to 48 hpi, respectively, was seen. No significant difference in the mean fold change of the Bax biomarker between groups or over time was detected, suggesting a possible protective role of limonin against necrosis rather than apoptosis in TBI. The concentration of limonin in the T2 group is 300 µM. The animal model used and the cohort design in all figures are adult zebrafish (*Danio rerio*)

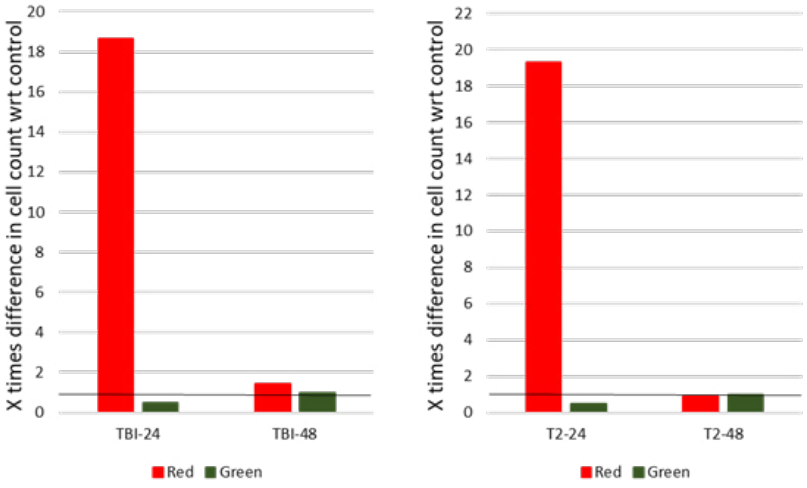

Figure 13. Acridine orange /ethidium bromide (AO/EB) staining-viability cell count trend in traumatic brain injury (TBI) and treated zebrafish groups at 24 hpi and 48 hpi
Green indicates viable cells (acridine orange-positive), while red indicates dead cells (ethidium bromide-positive)

Discussion

Limonin, a compound extracted from citrus seeds and fruits was previously known to cause chromosomal aberrations at higher concentrations (6). Thus, a toxicity assessment was performed to confirm therapeutic concentrations. The dosage range was successfully established, showing no general signs of toxicity such as skin irritation, changes in locomotion, appetite, or response to stimuli. The comet assay confirmed no nucleic acid breaks, validating the safety of the tested dosages.

Given that glutamate excitotoxicity, particularly through the activation of ionotropic glutamate receptors, is associated with post-traumatic seizures (PTS)(30), specific behaviors like corkscrew swimming, which pertain to motor control, were noted. Nuances such as the onset and duration of fin movements post-injury were also observed (30, 31).

The relationship between seizure and brain injury is complex and multifaceted, prompting this behavioral study. Despite limited direct evidence linking seizure-like activity duration to survival outcomes, our consistent stab injury method allowed for estimation of variations in the onset and duration of seizure-like activity. The T2 showed a visible reduction in flicks without detrimental effects on motility. Seizure-like activity, characterized by circling behavior, along with differential neuropsychiatric observations in the NTT, suggests neurotransmitter imbalance as a secondary consequence of the primary injury (32, 33). Exploratory behavior in the T2 group indicates no anxiety, implying no neurotransmitter imbalance.

Assessment of brain edema indicated that the T2 concentration of limonin effectively maintained vascular integrity and prevented excessive water accumulation, positioning it closest to the sham group (19). Limonin at 300 μM exhibited enhanced haemostatic properties, likely due to its ability to counteract hyperfibrinolysis, making it more effective compared to other concentrations in the TBI group.

Plant-derived bioactive compounds, particularly limonoids such as limonin, have been extensively studied for their antioxidant capacity. Limonin has shown promise in reducing levels of malondialdehyde (MDA) in conditions like colorectal adenocarcinoma (34). Moreover, limonin has been shown to increase sirtuin 1 levels, leading to antioxidative and anti-inflammatory effects through activation of the Nrf2 pathway and inhibition of the NF-κB inflammatory response (35). These effects have been observed in both in vitro and in vivo studies, following pre-incubation and treatment with limonin, particularly in cases of acetaminophen-induced hepatotoxicity (6). As expected, T2 concentrations show proof of being better at the molecular level of its known antioxidant nature in comparison with the others.

Histological staining with H&E provides a means to distinguish between immune cell types based on their morphological characteristics. The literature reports conflicting studies on the roles of different immune cell populations at various time points post-injury. For example, microglia cells initially promote neuroinflammation, which is crucial for clearing cellular debris following primary injury. However, prolonged activation and involvement of astrocytes may prove detrimental, potentially impeding proper synaptic rewiring (36). In this study, we conducted histopathological examination to assess changes in immune cell populations and microenvironmental structures across study groups, including observations at the 72 hpi, aiming to elucidate and validate the effects of limonin. Furthermore, the reduction in astrocytic cells in the T2 group at 24 hpi supports the hypothesis that limonin may shorten the overall recovery time by mitigating chronic inflammation, edema, and neuron-glial degeneration.

IL-6 shows high species homology between zebrafish and humans, validating its use as a pro-inflammatory cytokine (37). Upon comparison with the H&E section, the phenotypic outcomes appear promising for the T2 group at 72 hpi, aligning with the heightened IL-6 gene expression observed at 48 hpi in both the TBI and T2 groups, which ascertains the test concentrations' beneficial influence on the amplified and required inflammatory response.

No loss of myelination even with increased IL-6 levels at 48 hpi in the T2 group, suggesting no inflammation-mediated damage. This increases the likelihood of screening for biochemical and cellular homeostasis.

A recent study suggests that lipid droplet accumulation correlates with NLRP3 inflammasome activation, leading to increased mitochondrial ROS release and subsequent disruption of tight junctions in the choroid plexus, which can precipitate post-hemorrhagic hydrocephalus (39). The sequence of events following lipid droplet accumulation, such as immune cell chemotaxis to the injury site, is well documented. Studies have shown a correlation between TDP-43 and lipid droplets with microglial activation, and the elimination of these accumulations via granulin has been shown to revert microglia to their basal state, thereby preventing chronic inflammation and scarring (40). Given the systemic lipid-elimination properties (7), the role of limonin in modulating lipid dynamics in the CNS post-injury is investigated in this study, without making any a priori assumptions due to the existence of conflicting findings in the literature. T2 concentration of limonin effectively modulates lipid dynamics post-injury, as evidenced by histological analysis and assessment of the tissue microenvironment and myelination, validating optimal vascular integrity, reduced oxidative stress, and the absence of chronic inflammation.

As already established, there is a connection between TDP-43 and lipid accumulation. With specific quantitative or semiquantitative estimation of the protein, a reduction in this protein would suggest optimal regulation of the microglial state. However, to comprehend the fundamental mechanism underlying the interaction between the Bradford reagent and proteins, it is known that the reagent binds to basic amino acid residues. No specific group of proteins can be measured using this method. However, regarding the impact of limonin on protein concentration post-head injury, particularly at the critical time point of 48 hpi, it is hypothesized that limonin may help maintain basal tissue protein levels. This hypothesis is supported by results from assays of neuroinflammation and by the evident loss of tissue and vascular integrity observed at 48 hpi in both the TBI and the treated groups. T2 expressed a decrease in protein concentration. With an increase in IL-6 at 48 hpi in T2, this cytokine protein is also apparently not detected by means of the Bradford assay. Limonin, derived from pomelo seeds, has been shown to mitigate cellular apoptosis in neuron injury mediated by Aβ25-35 in PC12 cells by activating the PI3K/AKT Signaling Pathway (40). Leveraging this

knowledge, we investigated the most effective concentration for inducing its proposed neuroprotective effect post-injury, focusing on the T2 group, which emerged as optimal across multiple assays conducted in this study. With increased IL-6-mediated inflammatory signals at 48 hpi, the beneficial effect of limonin in mitigating cell degeneration is validated. Prevention of necrotic cell death is a notable observation in the T2 test group, along with a slight decrease in cell death compared with the TBI control.

AO/EB staining was validated using Bax marker expression, and, as expected, with a minute difference in cell death between groups due to the use of a wild-type model with natural regenerative capabilities, the mode of cell death following injury is a caveat. While previous similar studies have examined the effects of limonin in stroke models, focusing exclusively on isolated effects of pathological events, the current study demonstrates a comprehensive, holistic treatment option for TBI with limonin, covering multifaceted presentations of the condition. The impact of limonin treatment performed at a specific time frame of three days post injury can be translated to humans, and the model proposed can be efficiently used for pre-clinical screening of anti-inflammatory agents abiding by the 3Rs concept of animal experimentation.

Conclusion

Limonin T2 concentration emerges as a potent candidate for preconditioning or combination therapy in TBI, demonstrating efficacy in reducing oxidative stress, modulating neuroinflammatory responses, and promoting cellular survival and recovery. Future studies should focus on further elucidating the precise molecular mechanisms underlying limonin's protective effects and exploring its potential for clinical application in TBI management.

Acknowledgment

We acknowledge the Department of Biomedical Sciences, Sri Ramachandra Institute of Higher Education and Research, for providing infrastructure and lab facilities. The results described in this paper were part of a student's thesis.

Authors' Contributions

J M, L V designed the experiments; J M, MK S, S C performed experiments and collected data; J M, MK S discussed the results and strategy; L V Supervised, directed and managed the study; J M, L V, MK S Final approved the version to be published.

Conflicts of Interest

The authors have no relevant financial or non-financial interests to disclose.

Declaration

We have not used any AI tools or technologies to prepare this manuscript.

References

1. Gualdani R, Cavalluzzi MM, Lentini G, Habtemariam S. The chemistry and pharmacology of citrus limonoids. Molecules 2016; 21: 1530-1569.
2. Wang S-C, Yang Y, Liu J, Jiang A-D, Chu Z-X, Chen S-Y, *et al.* Discovery of novel limonin derivatives as potent anti-inflammatory and analgesic agents. Chin J Nat Med 2018; 16: 231-240.
3. Yang Y, Wang X, Zhu Q, Gong G, Luo D, Jiang A, *et al.* Synthesis and pharmacological evaluation of novel limonin derivatives as anti-inflammatory and analgesic agents with high water solubility. Bioorg Med Chem Lett 2014; 24:1851-1855.
4. Gerolino EF, Chierrito TPC, Filho AS, Souto ER, Gonçalves RAC, de Oliveira AJB. Evaluation of limonoid production in suspension cell culture of Citrus sinensis. Rev Bras Farmacogn 2015; 25: 455-461.
5. Hasegawa S, Miyake M. Biochemistry and biological functions of citrus limonoids. Food Rev Int 1996; 12: 413-435.
6. Fan S, Zhang C, Luo T, Wang J, Tang Y, Chen Z, *et al.* Limonin: A review of its pharmacology, toxicity, and pharmacokinetics. Molecules 2019; 24: 3679-3701.
7. Li Y, Yang M, Lin H, Yan W, Deng G, Ye H, *et al.* Limonin alleviates non-alcoholic fatty liver disease by reducing lipid accumulation, suppressing inflammation and oxidative stress. Front Pharmacol 2021; 12: 801730-801744.
8. Blennow K, Brody DL, Kochanek PM, Levin H, McKee A, Ribbers GM, *et al.* Traumatic brain injuries. Nat Rev Dis Primers 2016; 2: 16084.
9. Ng SY, Lee AYW. Traumatic brain injuries: Pathophysiology and potential therapeutic targets. Front Cell Neurosci 2019; 13: 528-551.
10. Shi K, Zhang J, Dong J-F, Shi F-D. Dissemination of brain inflammation in traumatic brain injury. Cell Mol Immunol 2019; 16: 523-530.
11. Iaccarino MA, Bhatnagar S, Zafonte R. Rehabilitation after traumatic brain injury. Handb Clin Neurol 2015; 127: 411-422.
12. Ghaddar B, Lübke L, Couret D, Rastegar S, Diotel N. Cellular mechanisms participating in brain repair of adult zebrafish and mammals after injury. Cells 2021; 10: 391-415.
13. Westerfield M. The zebrafish book: A guide for the laboratory use of zebrafish (*Danio rerio*). 4th ed. Eugene (OR): University of Oregon Press; 2000.
14. Jarvis RB, Knowles JF. DNA damage in zebrafish larvae induced by exposure to low-dose rate gamma-radiation: Detection by the alkaline comet assay. Mutat Res 2003; 541: 63-69.
15. März M, Schmidt R, Rastegar S, Strähle U. Regenerative response following stab injury in the adult zebrafish telencephalon. Dev Dyn 2011; 240: 2221-2231.
16. Schmidt R, Beil T, Strähle U, Rastegar S. Stab wound injury of the zebrafish adult telencephalon: A method to investigate vertebrate brain neurogenesis and regeneration. J Vis Exp 2014; 90: e51753-51761.
17. Michinaga S, Koyama Y. Pathogenesis of brain edema and investigation into anti-edema drugs. Int J Mol Sci 2015; 16: 9949-9975.
18. Cabrera-Aldana EE, Ruelas F, Aranda C, Rincon-Heredia R, Martínez-Cruz A, Reyes-Sánchez A, *et al.* Methylprednisolone administration following spinal cord injury reduces aquaporin 4 expression and exacerbates edema. Mediators Inflamm 2017; 2017: 4792932-4792939.
19. Mazzolini J, Chia K, Sieger D. Isolation and RNA extraction of neurons, macrophages and microglia from larval zebrafish brains. J Vis Exp 2018; 134-142.
20. Visavadiya NP, Patel SP, VanRooyen JL, Sullivan PG, Rabchevsky AG. Cellular and subcellular oxidative stress parameters following severe spinal cord injury. Redox Biol 2016; 8: 59-67.
21. Compton SJ, Jones CG. Mechanism of dye response and interference in the Bradford protein assay. Anal Biochem 1985; 151: 369-374.
22. Gotham SM, Fryer PJ, Paterson WR. The measurement of insoluble proteins using a modified Bradford assay. Anal Biochem 1988; 173: 353-358.
23. Cardiff RD, Miller CH, Munn RJ. Manual hematoxylin and eosin staining of mouse tissue sections. Cold Spring Harb Protoc 2014; 2014: 655-658.
24. Goto N. Discriminative staining methods for the nervous system: Luxol fast blue--periodic acid-Schiff--hematoxylin triple

stain and subsidiary staining methods. Stain Technol 1987; 62: 305-315.
25. Koopman R, Schaart G, Hesselink MK. Optimisation of oil red O staining permits combination with immunofluorescence and automated quantification of lipids. Histochem Cell Biol 2001; 116: 63-68.
26. Tiedeken JA, Ramsdell JS, Ramsdell AF. Developmental toxicity of domoic acid in zebrafish (Danio rerio). Neurotoxicol Teratol 2005; 27: 711-717.
27. Berg EM, Mrowka L, Bertuzzi M, Madrid D, Picton LD, El Manira A. Brainstem circuits encoding start, speed, and duration of swimming in adult zebrafish. Neuron 2023; 111: 372-386.
28. Hentig J, Campbell LJ, Cloghessy K, Lee M, Boggess W, Hyde DR. Prophylactic activation of Shh signaling attenuates TBI-induced seizures in zebrafish by modulating glutamate excitotoxicity through Eaat2a. Biomedicines 2021; 10: 32-50.
29. Turner KJ, Hawkins TA, Henriques PM, Valdivia LE, Bianco IH, Wilson SW, *et al*. A structural atlas of the developing zebrafish telencephalon based on spatially-restricted transgene expression. Front Neuroanat 2022; 16: 840924-840949.
30. McGuire JL, Ngwenya LB, McCullumsmith RE. Neurotransmitter changes after traumatic brain injury: an update for new treatment strategies. Mol Psychiatry 2019; 24: 995-1012.
31. Kalueff AV, Gebhardt M, Stewart AM, Cachat JM, Brimmer M, Chawla JS, *et al*. Towards a comprehensive catalog of zebrafish behavior 1.0 and beyond. Zebrafish 2013; 10: 70-86.
32. Ishak NIM, Mohamed S, Madzuki IN, Mustapha NM, Esa NM. Limonin modulated immune and inflammatory responses to suppress colorectal adenocarcinoma in mice model. Naunyn Schmiedebergs Arch Pharmacol 2021; 394: 1907-1915.
33. Yang R, Song C, Chen J, Zhou L, Jiang X, Cao X, *et al*. Limonin ameliorates acetaminophen-induced hepatotoxicity by activating Nrf2 antioxidative pathway and inhibiting NF-κB inflammatory response via upregulating Sirt1. Phytomedicine 2020; 69: 153211.
34. Liddelow SA, Guttenplan KA, Clarke LE, Bennett FC, Bohlen CJ, Schirmer L, *et al*. Neurotoxic reactive astrocytes are induced by activated microglia. Nature 2017; 541: 481-487.
35. Ollewagen T, Benecke RM, Smith C. High species homology potentiates quantitative inflammation profiling in zebrafish using immunofluorescence. Heliyon 2024; 10: e23635-23649.
36. Zhang Z, Guo P, Liang L, Jila S, Ru X, Zhang Q, *et al*. NLRP3-dependent lipid droplet formation contributes to posthemorrhagic hydrocephalus by increasing the permeability of the blood-cerebrospinal fluid barrier in the choroid plexus. Exp Mol Med 2023; 55: 574-586.
37. Zambusi A, Novoselc KT, Hutten S, Kalpazidou S, Koupourtidou C, Schieweck R, *et al*. TDP-43 condensates and lipid droplets regulate the reactivity of microglia and regeneration after traumatic brain injury. Nat Neurosci 2022; 25: 1608-1625.
38. Qiu Y, Yang J, Ma L, Song M, Liu G. Limonin isolated from pomelo seed antagonizes Aβ25-35-mediated neuron injury via PI3K/AKT signaling pathway by regulating cell apoptosis. Front Nutr 2022; 9: 879028-879039.